ME525 Applied Acoustics Lecture 21, Winter 2024
Introduction to ray theory

Peter H. Dahl, University of Washington

What is a ray? Ray fans and eigenrays

You should arrive at an immediate understanding of a ray by way of Fig. 1

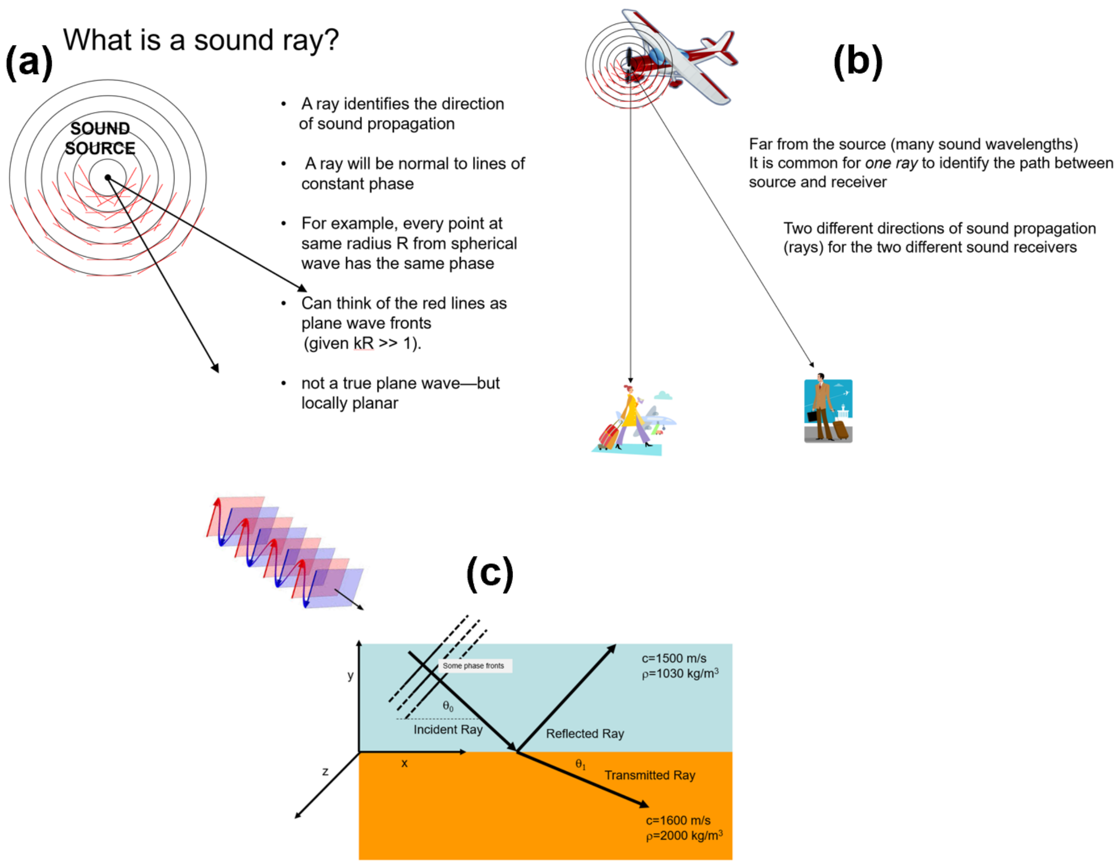

Figure 1: (a) Two rays (from an infinite number) emerging from a spherical source. The rays are perpendicular or normal to the lines of constant phase. The further away from source the more accurate this description becomes. (b) Sufficiently far from the source separate rays between the source and two different receivers are identified. When connecting the source to receiver in this manner these are known as *eigenrays*. (c) By now a familiar picture: a ray of particular grazing angle θ_0 encounters a boundary.

In the analysis of the plane wave reflection coefficient you encountered Snell's law. For the specification of θ_0, θ_1 in Fig. 1 (c), Snell's laws is

$$\frac{\cos\theta_0}{c_0} = \frac{\cos\theta_1}{c_1} \tag{1}$$

As mentioned before, it pays to memorize Snell's law. Everything about ray theory will follow from Snell's law.

Figure 1 (c) showed the reflection process between two mean of differing characteristic impedance or $\rho_0 c$. Still, there was a *refraction* process as shown by the change in angle from θ_0 to θ_1. In the air (or atmosphere extending several km in altitude) and underwater, the speed of sound can vary significantly. The essence of ray theory is all about refraction caused by these changes, where a ray horizontal angle changes from one propagation angle another, as θ_0 to θ_1 when the sound speed changes from c_0 to c_1, governed, of course, by Snell's law.

For your first introduction to rays, think of them in a 2D sense: one dimension z is depth e.g. as applied to underwater sound, or altitude as applied to airborne sound; sound speed is allowed to vary as $c(z)$. The other dimension r is range. Conventional 2D ray theory will determine how a ray travels in this $r - z$ plane. Figure 2 illustrates this. In the upper plot $c(z)$ is constant; thus a ray starting at angle θ_0 remains at θ_0 and there is no refraction. In the second plot $c(z)$ decreases with depth; rays will tend to refract downward following Snell's law. Memorize: "rays want to head towards the lower sound speed". In the third plot $c(z)$ increases with depth and the opposite happens. Finally in the lower plot a combination of increasing and decreasing $c(z)$ is in effect; a ray launched a this precise point of the sound speed maximum will tend to refract both upward or downward–but there is no way for sound to move straight ahead. A shadow zone develops where sound intensity is reduced. Qualitatively this will be indicated by a lower density of rays (we'll see many more examples of this effect).

Ray fans are "fans" of rays "launched" from a sound source location; each ray has a different ray launch (horizontal) angle θ_0. Take the sound speed at the source location as c_0, then Snell's law dictates how the ray responds going forward from that point. In fact, the ratio $\frac{\cos\theta_0}{c_0}$ will forever stick with that ray, and this value is known as the *ray parameter* for a given ray. If this ray encounters a new speed c_1 then of course Snell's law determines the new angle θ_1.

Ray fans give a useful qualitative view of how sound propagates away from a source, and show where shadow regions (ray density low) , or convergence regions (ray density high). Figure 3 depicts a fan of rays emitted from a source at depth 40 m over a spread launch angles of $\pm 40°$, for conditions representing a summer sound speed profile off the coast of New England. At range $\sim$ 150 m, depth $\sim$ 45 m, there is lower density of rays, at range 200-300 m, depth $\sim$ 20 to 30 m, there is a higher density of rays, which influences the overall sound intensity received at these locations.

Observe that several rays, e.g. $\sim$ at depth 10 m, range 200 m, have reached a horizontal angle of $0°$ and have turned around to eventually reflect from the sea bed. Upon reflection these rays will again reach precisely the same turn-around depth, e.g., some at about range 900 m, with the process repeated. A group of such rays, all having similar turn-around depths and ranges, forms a feature known as a *caustic*, represented here as the darker curve developing at depth $\sim$ 25 m, between ranges 200-500 m.

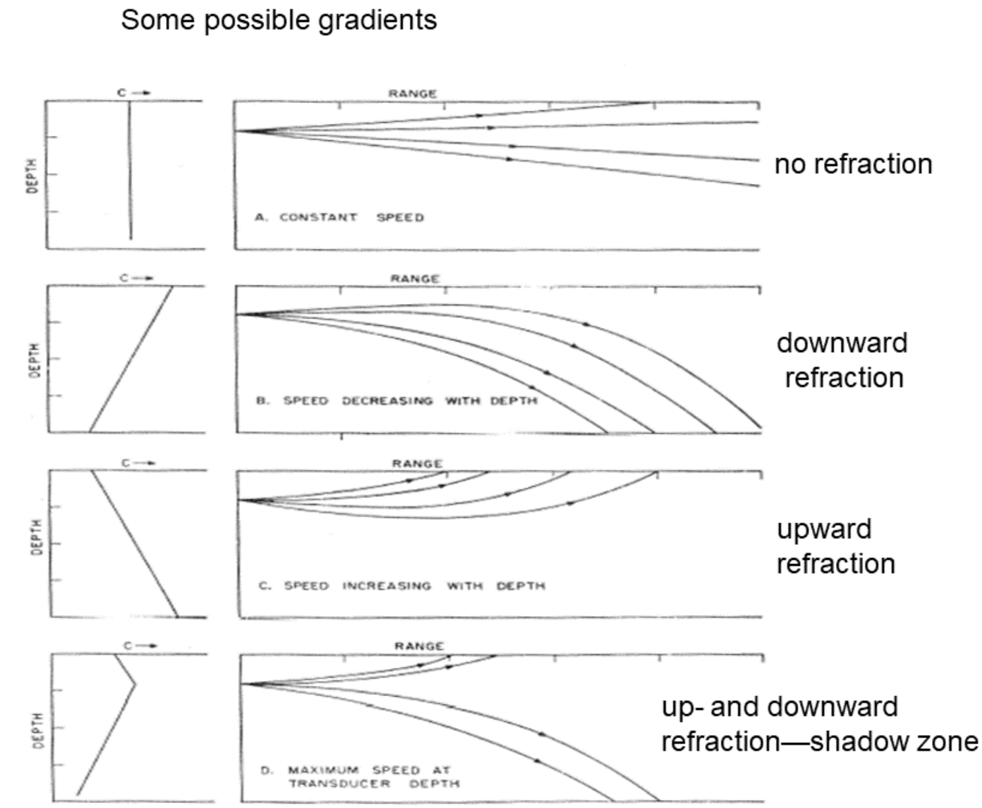

Figure 2: Upper plot: $c(z)$ is constant a ray starting at angle θ_0 remains at θ_0 and there is no refraction. Second plot: $c(z)$ decreases with depth; rays refract downward following Snell's law. Third plot: $c(z)$ increases with depth and the opposite happens. Lower plot: a combination of increasing and decreasing $c(z)$ is in effect; a ray launched a this precise point of the sound speed maximum will tend to refract both upward or downward–but there no way for sound to move straight ahead.

Often we start with ray fan to get qualitative feel for the sound propagation conditions. The next step might be to select only those rays that connect source to receiver. These are *eigenrays* and Fig. 4 shows a set of five eigenrays that connect source and receiver for an experiment in the East China Sea. Finding eigenrays is achieved in some approximate sense, by finding a ray that reached depth $z \pm \Delta z$ and range $r \pm \Delta r$, where one experiments with $\Delta z, \Delta r$ until a suitable result found. The eigenray problem is somewhat more difficult because of this optimization task, but computation of ray fans or eigenrays is still relatively straight forward.

In underwater acoustics (as with many other applications in acoustics) sound from source reaches a receiver via multiple pathways. Figure 4 also shows what is known as multipath propagation. The direct path (red) arrives first, with launch angle ($theta_0$) of 1.3° (positive angle below horizontal). The next arrival is the eigenray (green) reflecting from the sea surface with launch angle -9.4°. Though not shown, the sound speed profile $c(z)$, must be such that $c(z)$ is decreasing for depths below the source depth because the direct path eigenray is refracting downwards. Other arrivals can seen in the pulse structure which correspond one-to-one to the eigenrays (though the color coding may be off).

Finally, an additional output from ray theory–and in some cases the crucial output–is the travel time over the length the ray. In this example the direct path arrived in 302 ms (range 0.46 km), and the surface path arrived +3.2 ms later, etc. Accurate ray travel time is essential in the study of acoustic tomography where the arrival times of rays traveling over the span oceanic scales yield information about the intervening sound speed between source and receiver which in turn provides information on global ocean temperature.

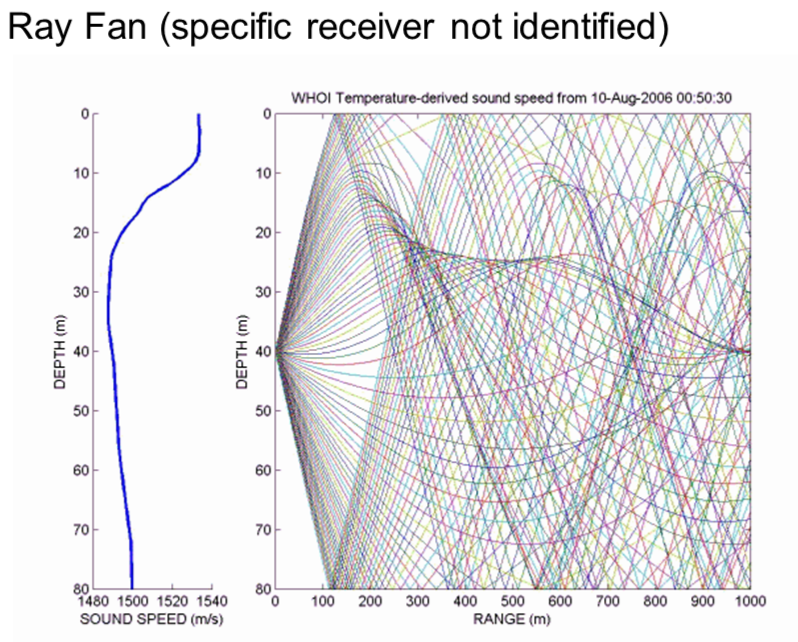

Figure 3: A fan of rays emitted from a source at depth 40 m over a launch angle spread of $\pm 40°$, for conditions representing a summer sound speed profile of the coast of New England. At range $\sim$ 150 m, depth $\sim$ 45 m, there is lower density of rays, at range 200-300 m, depth $\sim$ 20 to 30 m, there is a higher density of rays, which influences the overall sound intensity received at these locations.

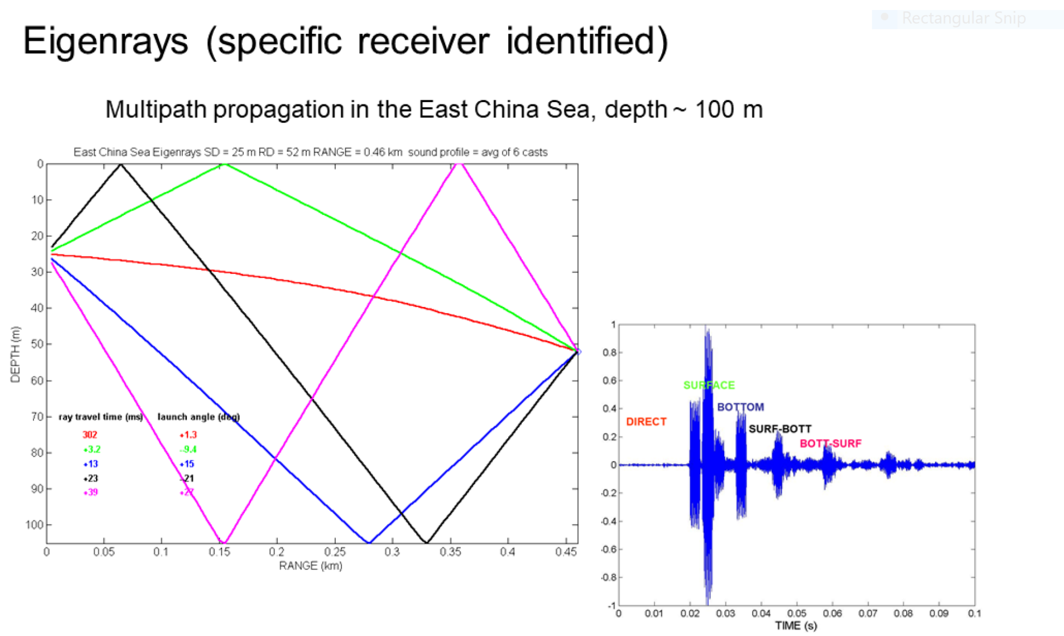

Figure 4: Multipath propagation in the East China Sea. The direct path (red) with launch angle +1.3° and having no reflections reached the receiver down range at 0.46 km, in 302 ms. Four other paths (eigenrays) are shown along with estimated travel times relative to the direct path. These arrival times correspond well pulse shown on the right (time axis is relative).

The linear sound speed gradient

One can make considerable quick progress with ray theory by assuming the sound speed c varies in a linear manner with depth z, as in $g = \frac{dc}{dz}$. The key property in this case is that refraction will be manifested by rays following arcs of a circle, for which the radius of curvature goes as the inverse of the gradient g. (This should make sense intuitively: with no variation $g = 0$ and radius of curvature is infinite, representing a straight line.) Figure 5 summarizes a set handy equations for ray travel time ΔT, radius of curvature R_c, change in range ΔR and change in depth Δz for a linear sound speed gradient g.

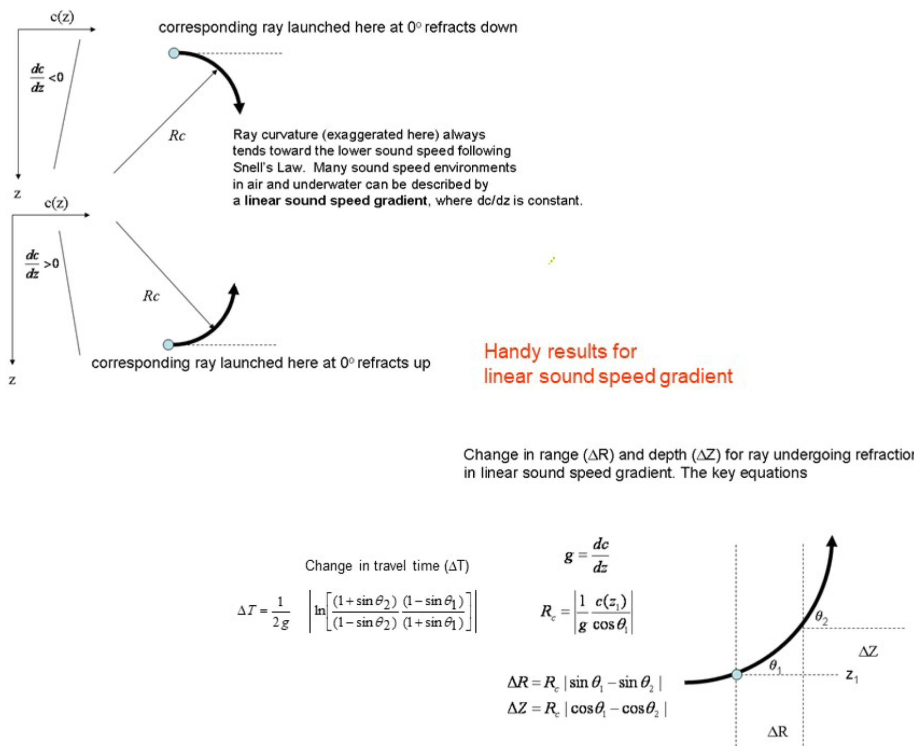

Figure 5: Refraction of rays with radius of curvature R_c due to propagation through a linear sound speed gradient, and handy set of equations for finding ray travel time ΔT, radius of curvature, change in range ΔR and change in depth Δz for a linear sound speed gradient g. Note: with $g = \frac{dc}{dz}$ then g can be either negative or positive, so use $|g|$ in the expressions for R_c and ΔT.

Example of linear sound speed approximations for ray theory applied to sound in air

An example of how one might use these linear profile ray equations comes from a problem we paraphrase from Garrett (2017). A highway engineer is tasked with measuring road noise at range 150 from the road. Data for sound speed at 0.5 m above ground (342.8 m/s) and at 5 m (341.3 m/s), indicates a more typical reduction in temperature with height above ground (i.e., not a temperature inversion), and from this data we estimate the gradient $|g| = 0.333$ s^{-1}.

The objective is to measure the sound emerging from cars with launch angle $0°$ as caused by tire noise (the largest source of car noise). Given the sound speed data, the engineer knows that the $0°$ ray will refract upwards, towards the lower sound speed region. Thus how high above the ground should the microphone be placed at range 150 m to have a good measurement of sound that was emitted horizontally from tires?

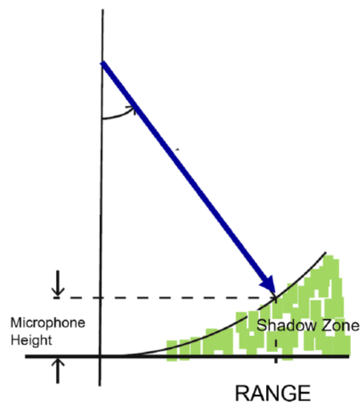

Figure 6: Shadow zone (colored region) for the horizontal ray caused by typical near-ground temperature gradient, and radius of curvature for this ray.

The decreasing sound speed with height above ground means upward refracting rays will have a constant radius of curvature that goes as the inverse of the gradient g (Fig. 6), and a shadow zone along ground level will develop. We find $R_c = |342.8/.333|$ = 1029 m, given the gradient estimate for g and that the initial launch angle $0°$. The range ΔR is established to be 150 m, which determines θ_2 as $8.4°$. Thus, following equations in Fig. 5 estimate the microphone height Δz to be about 11 m to avoid being placed within the shadow zone.

The next four figures provide additional examples of ray theory as used in underwater or upper atmosphere environments. Only brief commentary is provided in each caption. You should be able to intuit the basic look of each example.

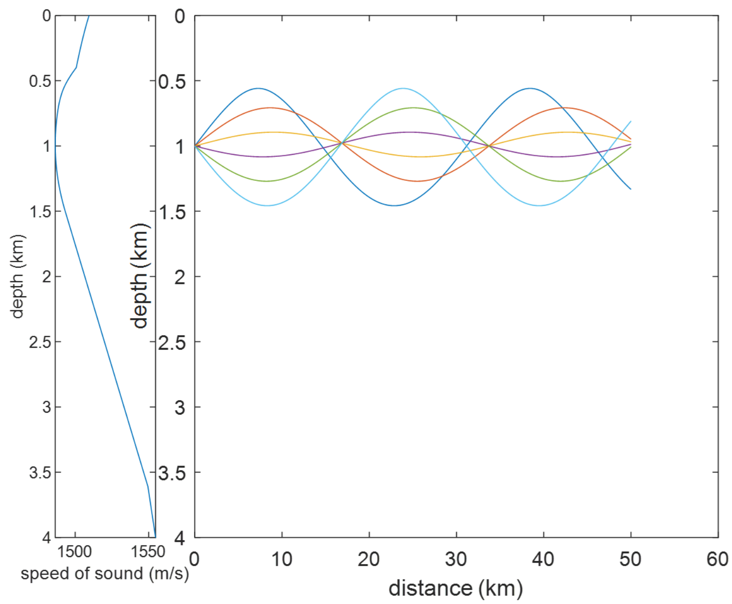

Figure 7: Deep water sound speed profile $c(z)$ (left) is known as a Munk profile after the celebrated oceanographer Walter Munk. A minimum in the $c(z)$ is found at depth of 1000 m. Five rays (right) are launched at this depth with launch angles θ_0 within $\pm 5°$.

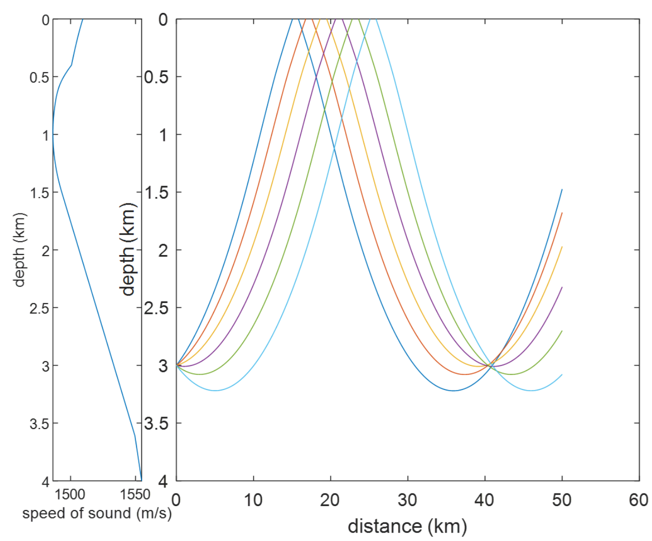

Figure 8: Based on the same Munk profile, five rays are launched at depth 3000 m with launch angles θ_0 within $\pm 5°$

References

H. Medwin and C. S. Clay *Fundamentals of Acoustical Oceanography*,(Academic Press, San Diego, CA, 1998)

S. L. Garrett, *Understanding Acoustics*, (Springer, Acoustical Society of America Press, 2017).

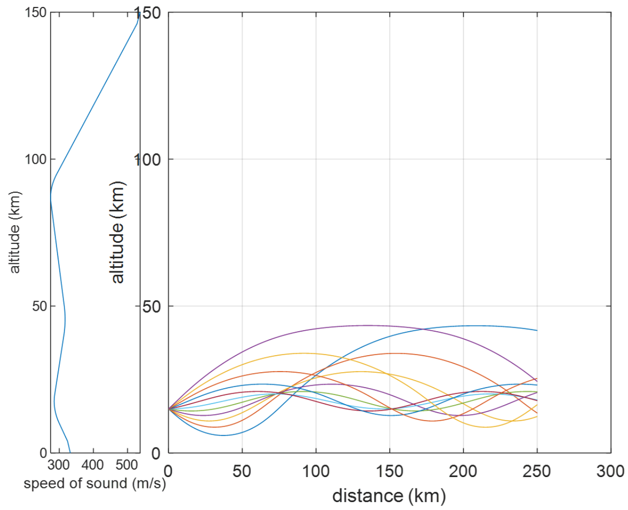

Figure 9: An atmospheric profile for $c(z)$ (left) shows a typical variation in sound speed in air extending from sea level to a height of 150 km. A local minimum in $c(z)$ occurs at an altitude of 15 km, and 11 rays (right) are launched at this altitude with launch angles θ_0 within $\pm 25°$.

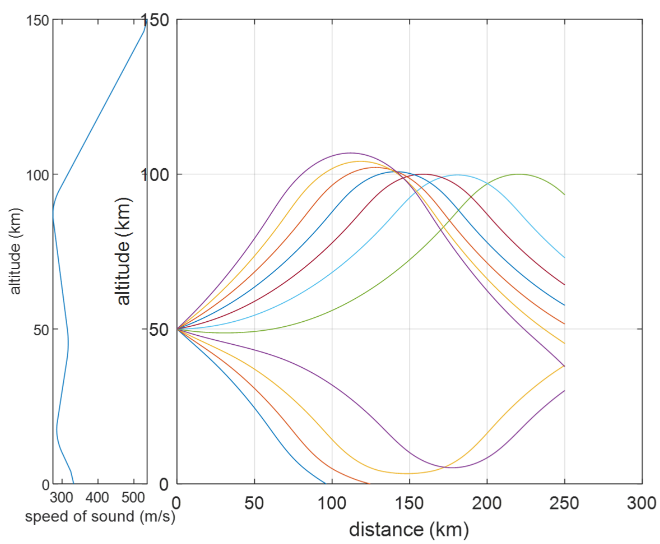

Figure 10: An atmospheric profile for $c(z)$ (left) shows a typical variation in sound speed in air extending from sea level to a height of 150 km. A local maximum in $c(z)$ occurs at an altitude of 50 km, and 11 rays (right) are launched at this altitude with launch angles θ_0 within $\pm 25°$.

ME525 Applied Acoustics Lecture 22, Winter 2024
Using ray theory approximations based on linear gradients

Peter H. Dahl, University of Washington

Ray equations based on the linear sound speed gradient

Two sound speed profiles that can be described (approximately) by linear gradients (Fig. 1) are: (1) a canonical high-latitude (arctic) profile that starts at $c(0) = 1440$ m/s and increases 80 m/s over the 5000 m depth, thus the gradient $g = 0.016$ s^{-1}, and (2) a canonical mid-latitude profile that has $c(0) = 1490$ m/s, and decreases linearly to $c(1000) = 1456$ m/s, thus the gradient $g = 0.034$ s^{-1}, after 1000 m the $c(z)$ continues to increase with $g = 0.016$ s^{-1}. The decrease in speed from the surface to 1000 m is due to a *thermocline*, the increase thereafter at rate $g = 0.016$ is the result of increasing hydrostatic pressure.

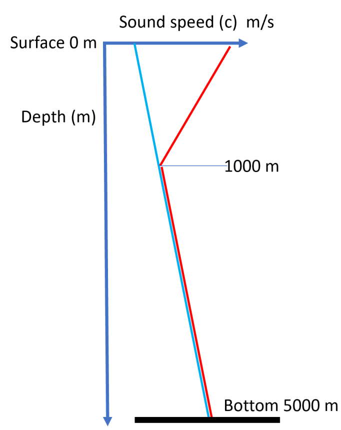

Figure 1: Underwater sound speed for arctic or high latitude (blue) and mid-latitude waters (red)

Now suppose there is preliminary design task for sonar system to be deployed at depth 500 m in waters described by the high-latitude (arctic) case. There is an operational goal to have the sound remain completely in the water column, i.e., does not undergo reflection from the seabed which can result in energy loss particularly if the grazing angle is greater than the critical angle. Thus, to cover the entire depth and also avoid reflection from the seabed, a ray must reach a *vertex* point at or near the seabed, where the ray has a reached a grazing angle of 0° at (or near) the seabed after which it will refract upwards. At this vertex point the sound speed c_v equals 1520 m/s, i.e., the sound speed at depth 5000 m. What is the launch angle for this ray? At depth 500 m the sound speed c equals 1448 m/s; define this speed as c_0. Call the launch angle,θ_v and find it directly from

Snell's law:

$$\frac{\cos\theta_v}{c_0} = \frac{1}{c_v} \tag{1}$$

and equals 17.7°. From this we actually now that any ray with launch angle ± 17.7° will stay completely within the water column. For example, such information may serve as a design guide for sonar array for which the vertical angle is limited to ± 18°.

Such a ray will have a *cycle distance* – in this case the ray is directed towards the sea surface, reflect, then directed down to the vertex depth (about 5000 m), and refracts back up, repeat. We can find these distances in a simple, approximate way as follows. Take the first segment from source depth 500 m to the surface. Find the radius of curvature R_c (refer to Fig. 3 of Lecture 21) where the applicable values are $R_c = |\frac{1448}{g\cos 17.7°}|$, setting R_c to about 95 km. Next find ΔR or the range from source at 500 m to the surface, where $\Delta R = R_c|\sin 17.7° - \sin 18.7°|$ or about 1.6 km, and the $18.7°$ surface grazing angle is always found via Snell's law.

Next, at the surface this ray reflects and heads down to near the seabed, it will take another 1.6 km to get to the depth 500 m. After 500 m, it continues downward while continually lowering its grazing angle until vertex is reached. The range from depth 500 m to the vertex is found as $\Delta R = R_c|\sin 17.7° - \sin 0°|$, or about 29 km. Now another 29 km to arrive back at the depth 500 m, giving the cycle distance for this ray as 3.2 km plus 58 km or about 61 km. A ray fan for this profile (Fig. 2) shows the 17.7° ray (thick line) launched at depth 500 m with cycle distance nicely consistent with ∼ 61 km estimate made here by considerably simpler means.

Having found this vertical angle angular range, ∼ ± 18°, the result can be incorporated into the design goal for a sonar, say mounted on front of an autonomous underwater vehicle (AUV). The design calls for the transmitting aperture to be a disk of diameter D (Fig. 2) and it is desired to have D to equal 0.3 m. The design frequency is not yet set. But the the effective beam width of the sonar will be approximately $60\lambda/D$ measured in deg (see Figs. 6 and 7 of Lecture 13) where λ is wavelength of sound. Now setting $36° = 60\lambda/D$ establishes the design frequency of about 8 kHz. All very approximate–but this is how preliminary "back of the envelope" ideas develop. More refined techniques will likely not very too much from this result.

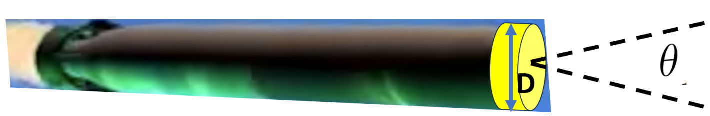

Figure 2: Sonar preliminary design task: Sonar (yellow) mounted on an Autonomous Underwater Vehicle (AUS), is circular array of diameter D with beamwidth θ.

Repeat the exercise using the mid-latitude case, again with a sonar system at depth 500 m with same goal of launching a ray that remains completely in the water column. In this case the sound speed at depth 500 m is $c_0 = 1473$ m/s. The vertex speed c_v at depth 5000 m is also 1520 m/s, and

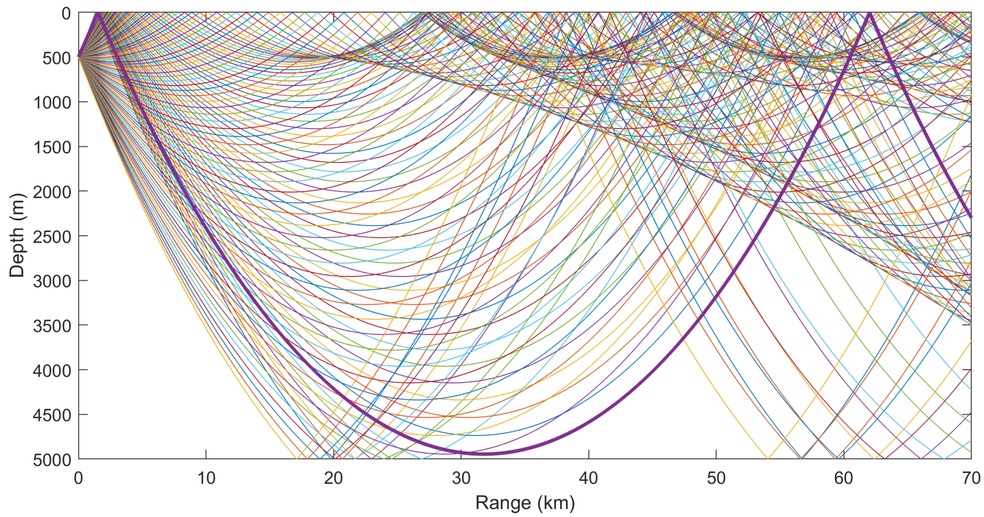

Figure 3: Ray fan and one of two limiting rays (thick line) launched at 17.7° at depth 500 m for the arctic or high latitude sound speed profile (Fig. 1). The cycle distance is $\sim$ 61 km. Second limiting ray, -17.7°, would give similar distance.

from Snell's law we find θ_v equal to $\pm$ 14.3°. Notice: this ray traversed two sound speed gradients to get to depth 5000 m, one downward-refracting and one upward refracting. Still, one simple Snell's law application gave us θ_v.

This ray thus now refracts downward as it heads up toward the sea surface where the speed is 1490 m/s, and Snell's puts angle there at 11.4°. The R_c for this segment must take into account the higher gradient ($g = 0.034$), with $R_c = |\frac{1473}{g \cos 14.3°}|$ equal to about 44.7 km. The range from source depth to surface is thus $\Delta R = R_c|\sin 14.3° - \sin 11.4°|$ or about 2.2 km.

The ray reflects and takes another 2.2 km to get back to depth 500 m, where the grazing angle has again reached 14.3°. From there the ray must go another 500 m in depth after which the gradient of sound speed profile will change at depth 1000 m. The sound speed at 1000 m is 1456 m/s, so the ray must have reached a grazing angle of 16.7° (Snell's law), and the horizontal distance for this phase is $\Delta R = R_c|\sin 14.3° - \sin 16.7°|$ or about 1.8 km.

From here the ray continues downward to the vertex depth of about 5000 m. The gradient has changed back to $g = 0.016$ and $R_c = |\frac{1456}{g \cos 16.7°}|$ or about 95 km. Thus the range from depth 1000 m to 5000 m is $\Delta R = R_c|\sin 16.7° - \sin 0°|$ or 27 km. Adding these ranges yields 4.4 km + 3.6 km + 54 km, or about 62 km. A ray fan for this profile (Fig. 4) shows the $\pm 14.3°$ rays (thick lines) launched at depth 500 m with cycle distance also consistent with our simple estimate.

Of course the sound speed profiles in Fig. 1 are idealized in two ways. The first being that sound speed $c(z)$ can change both with range and time (more on time variation below), the second being that water depth or bathymetry can change with range. Figure 5 illustrates this with data taken from the Marginal Ice Zone (MIZ) . In the above two examples we have been studying *RSR paths* or a ray path that is refracted-surface-reflected, and our goal was to find the deepest RSR path.

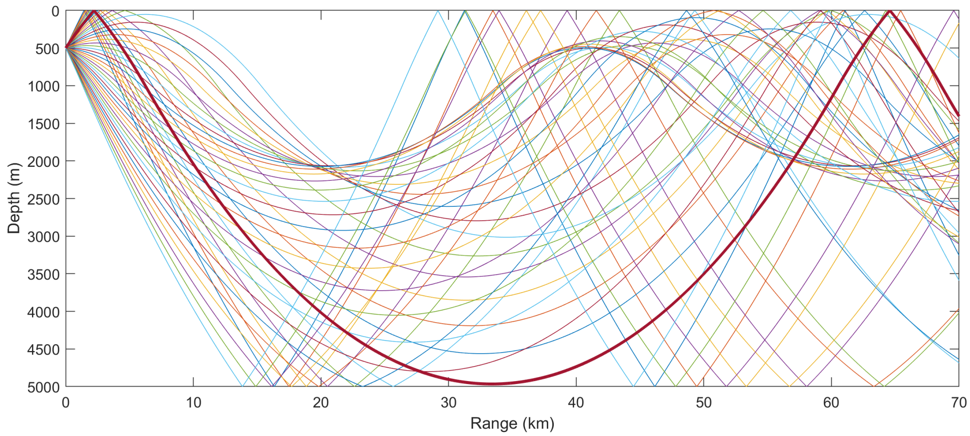

Figure 4: Ray fan and one of two limiting rays (thick line) launched at $14.3°$at depth 500 m for the mid-latitude sound speed profile (Fig. 1). The cycle distance is $\sim$ 62 km. Notice the existence of caustics where ray converge, and shadow zones, where ray coverage is less. Second limiting ray, -14.3°, would give similar distance.

Additional , and more shallow, RSR paths are shown for the MIZ condition in Fig. 5.

Other examples of on use of ray theory

Figure 6 (left) conveys a variation in measured sound speed versus depth and time $c(z;t)$ over a few hour period, with the largest variation occurring over the depth range 5 to 40 m as indicated by the gray shaded area. A set of eigenrays (right) for two receiver depths corresponding to $c(z;t)$ shows the sensitivity of the eigenrays to such variation. Notice that the direct path eigenray to the more shallow receiver shows the most variation even though a surface reflected path traversed the same region of high sound speed variation. As a general rule, rays with lower grazing angle with respect to the horizontal as in this direct path ray, will be more sensitive to changes in sound speed.

In Fig. 7, a simple demonstration of the effect of temperature inversion is shown for the case of hillside community and sound source below it. (This time of year temperature inversions are more frequent and you may on occasion experience more loudness from aircraft.) Ray theory provides an easy qualitative description of the effect of increasing sound speed with altitude owing to the inversion, with the hillside community likely experiencing higher noise levels from the noise source below.

This concludes our discussion of rays. If sound or acoustics is involved in your future career path, rays will invariably enter the picture. Likely you will not be writing your own complicated (and probably clunky) matlab program which I once did to make Figs. 2, 3 and 5 (I also produced Fig. 4 as a grad student but that was with a program from seismology) , but some aspect of refraction and rays will always be there. So, memorize Snell's law. We go on next to the formal underwater waveguide. Of course rays play a big part there but our focus for the remainder of the

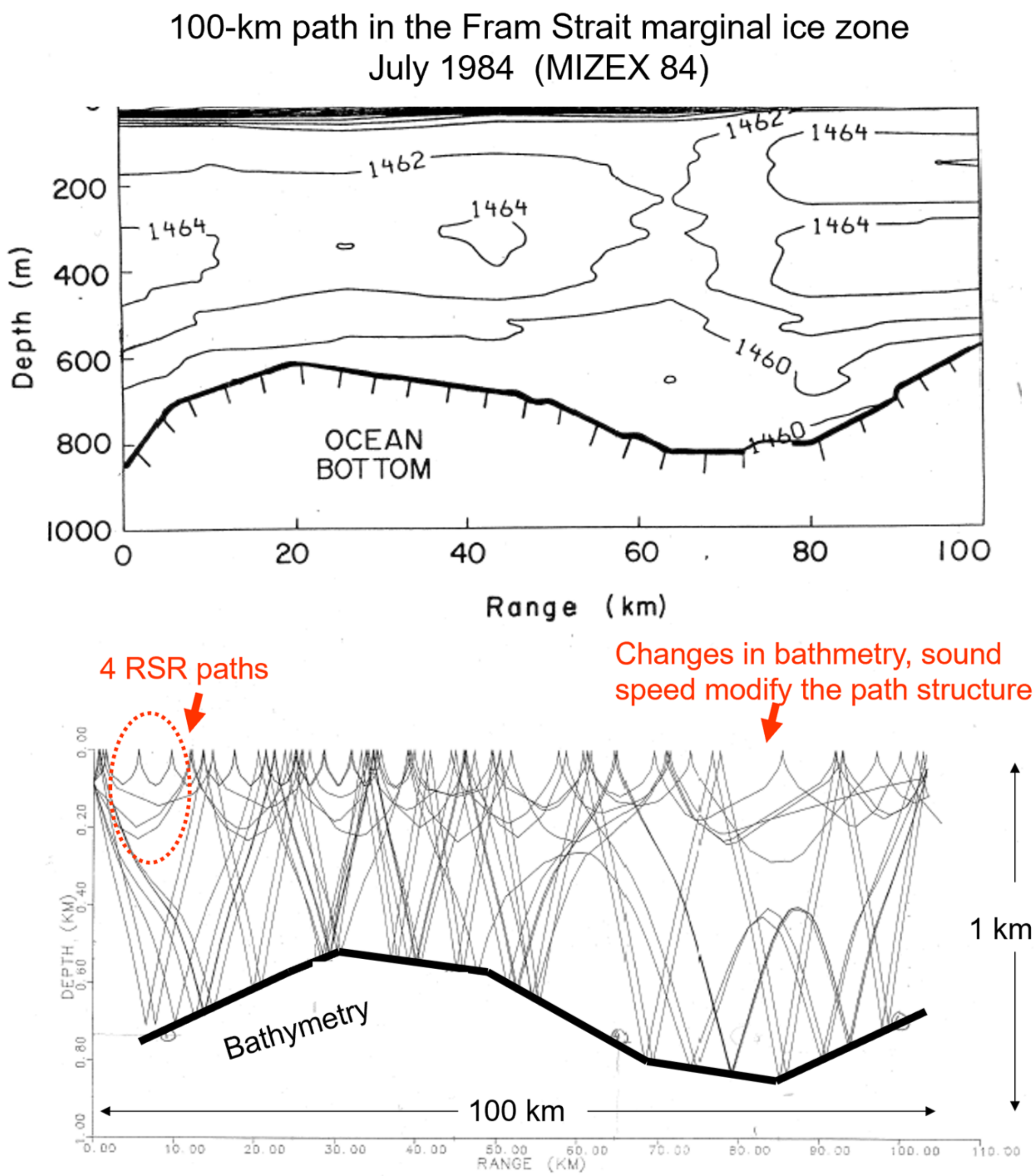

Figure 5: Top: Range-dependent bathymetry and sound speed profile over 100 km path in the Marginal Ice Zone. Figure from Dahl, Baggeroer, Mikhalevsky and Dyer, J. Acoust. Soc. Am., 1988. Not evident in the figure is the change in sound speed over the top 50-m from from about 1440 m/s to 1460 m/s. Bottom: rays computed for the above sound speed structure using a range-dependent ray trace program responsive to both changing depth and sound speed with range.

course will be on the method of normal modes.

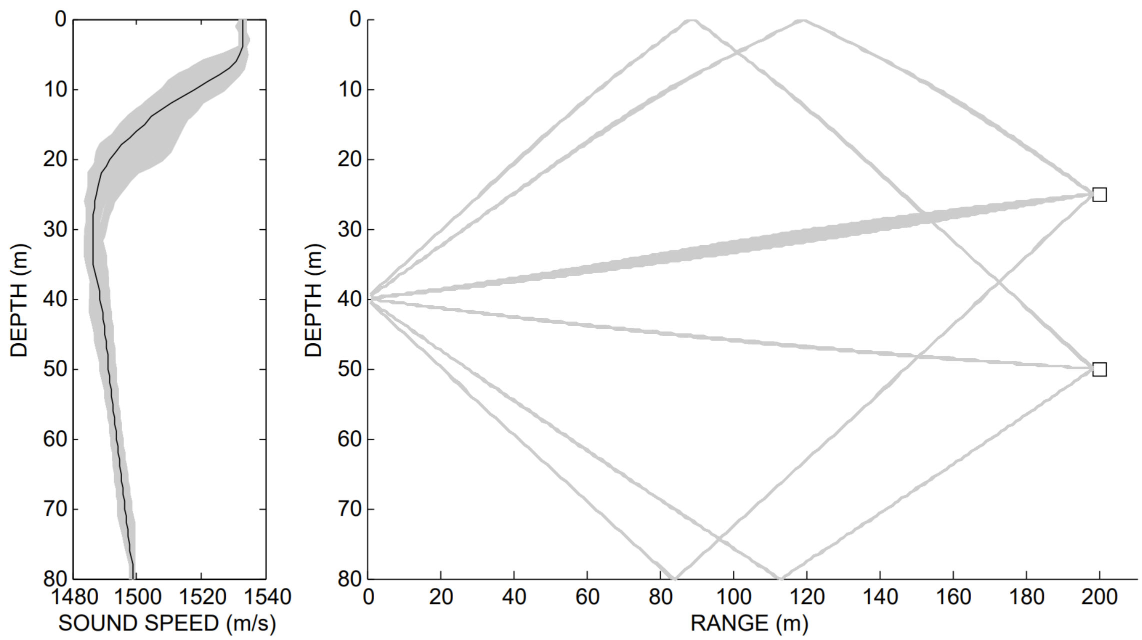

Figure 6: Left: Sound speed profile and typical variation over time due fluctuating oceanographic conditions. Right: Eigenrays computed for two receiver depths for spread of sound speed profiles. The direct path for the upper receiver is more sensitive to the fluctuating sound speed profile.

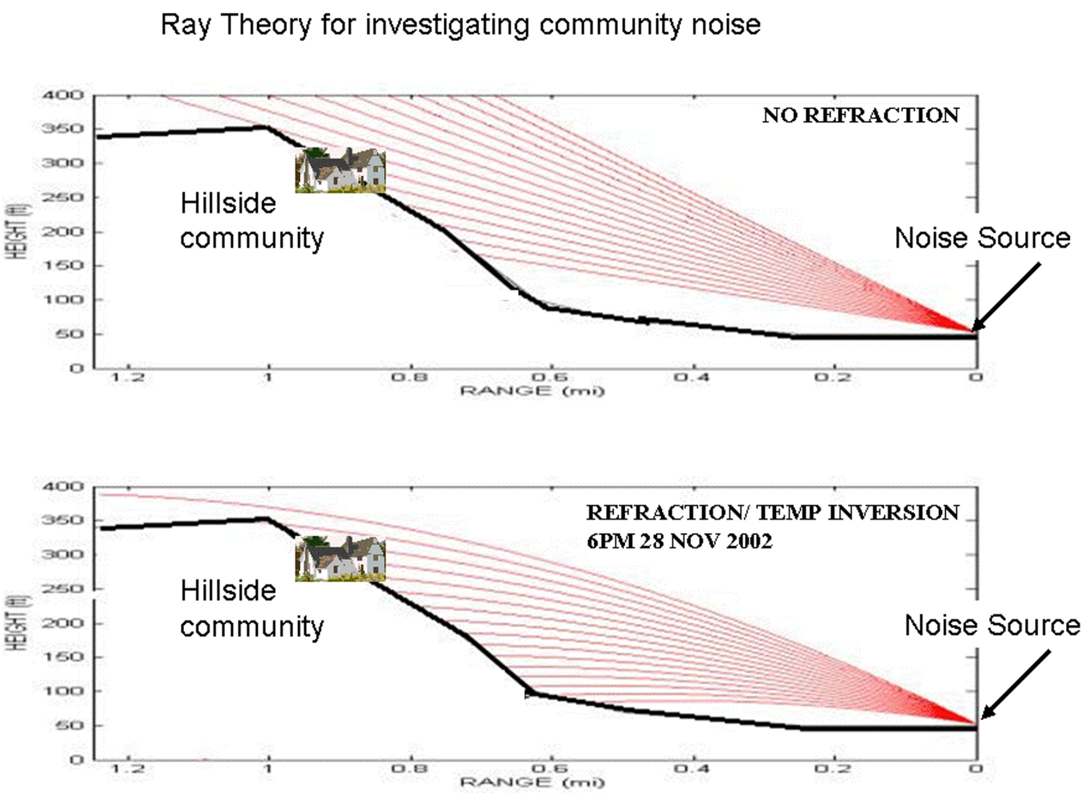

Figure 7: Top: sound rays emerging from a noise source traversing through air medium with constant sound speed. Bottom: temperature inversion causes sound speed to increase with altitude and rays from sound source are refracted downward; in this case the concentration of rays, hence loudness, at the hillside community has increased.